Lab on a Chip

Cite this: *Lab Chip*, 2012, **12**, 4449–4454

www.rsc.org/loc

PAPER

All-optical microfluidic chips for reconfigurable dielectrophoretic trapping through SLM light induced patterning†

Lisa Miccio,*[a] Pasquale Memmolo,[ab] Simonetta Grilli[a] and Pietro Ferraro[a]

Received 11th July 2012, Accepted 2nd August 2012
DOI: 10.1039/c2lc40789b

We explore a novel approach for fabricating polymeric microfluidic-channelled dielectrophoretic (DEP) chips by direct laser projection through a holographic Spatial-Light-Modulator (SLM) onto photorefractive crystal substrates. As the first step, an all-optical mould-free approach was used to fabricate the PDMS microfluidic channel, by exploiting the light induced space charge field in Fe-doped lithium niobate crystals, with the aim of integrating a microfluidic channel directly onto the functionalized substrate. Subsequently, as the second step, geometrical flexible DEP traps can be created onto the substrate by the same SLM holographic projection system. The experimental verification shows the trapping of flowing carbon nanotubes (CNTs) and the formation of chaining effects with graphite nanofibers. The main feature of the SLM is the ability to display an arbitrary light intensity pattern that is used here for fabricating the channels. Moreover, the reconfigurable trapping of CNTs is possible simply by the optical writing/erasing of various light intensity patterns projected by the SLM.

Introduction

The manipulation of nano and microparticles is a fundamental issue in microfluidic technology and biotechnology applications. One significant approach is based on dielectrophoresis (DEP) since it can be easily integrated into lab-on-a-chip devices.[1,2] In DEP processes a force is exerted on dielectric particles in the presence of non-uniform electric fields, thus giving the possibility of manipulating particles. For example, the separation of cells by DEP exploits the polarization of cells in non-uniform electrical fields. In fact, DEP forces depend on factors such as the electrical properties of the cell membrane and cytoplasm as well as cell size. Consequently, on-chip DEP devices have been developed for separating cancer cells, based on differences in the response of the cells to electric fields.[3,4] On the other hand, DEP is a key technological tool for orienting and positioning carbon nanotubes. Pioneering work in the electric-field assisted manipulation of CNT (carbon nanotube) bundles enabled the assessment of DEP as a promising tool in nanotechnology.[5–7] The assembling of CNTs for nanosensing under DEP force has been achieved.[8] However, the technological problems associated with the fabrication of the electrodes and with the need to achieve a rapid prototyping of DEP-based lab-on-a-chip devices has stimulated the investigation towards simpler and more versatile on-chip DEP concepts. Recently, DEP cell manipulation using electrodes on reusable printed circuit boards has been demonstrated to make DEP more affordable and convenient for on-chip applications.[9] Moreover, separation of live and dead bacteria was demonstrated with insulator-based dielectrophoresis (i-DEP). Interestingly, in i-DEP an electrode-free configuration has been developed to avoid the need for electrode fabrication and to overcome the issues connected with the compatibility of different materials. In addition, lately the i-DEP concept has been extended to three-dimensional dielectrophoresis.[10] Furthermore, the versatility and flexibility of optically switched dielectrophoresis (ODEP) has been also exploited for the manipulation and assembly of multi-particles.[11] Recently, the possibility to integrate DEP based devices with light trapping has been investigated in order to manipulate individual nanowires.[12] Other research activities have considered electrode-free DEP approaches that involve ferroelectric crystals and their properties. DEP trapping of microparticles was demonstrated on Fe-doped lithium niobate (LN) photorefractive crystals through light induced space charge fields.[13] Furthermore, recently, DEP was demonstrated by exploiting the pyroelectric effect in LN substrates. The DEP effect was induced by the pyroelectric space charge fields that led to the possibility of obtaining liquid and tuneable microlens arrays,[14] DEP trapping of fluorescent particles and polystyrene spheres,[15] or even self-assembly and the curing of two-dimensional periodic PDMS structures by a novel surface charge lithography.[16] The so called Pyro-DEP or Pyro-EHD (electrohydrodynamic effect) added 3D capability in the manipulation of liquids.[17–20] However, one of the very attractive advantages of the "photorefractive-approach", over

[a]*Istituto Nazionale di Ottica del CNR (CNR-INO), U.O.S. di Napoli, Via Campi Flegrei, 34 - 80078, Pozzuoli (NA), Italy. E-mail: lisa.miccio@ino.it; Fax: +390818675118; Tel: +390818675040*
[b]*Center for Advanced Biomaterials for Health Care@CRIB, Istituto Italiano di Tecnologia, P.le Tecchio 80, 80125 Napoli, Italy*
† Electronic supplementary information (ESI) available. See DOI: 10.1039/c2lc40789b

all of the methods described above, is that the electric field distribution is induced by light exposure. Another important advantage is that the space charge distribution can be erased and re-written making the DEP geometry reconfigurable with, in principle, any geometry.[21,22] In addition, with respect to ODEP, the distribution of electric charges can be considered stable and permanent until it is erased by intentional and successive uniform exposure to a light intensity distribution.

Here we report, for the first time, the possibility of fabricating microfluidic chips directly onto LN crystals using the photorefractive effect. We also demonstrate that the chips can be employed for reconfigurable particle trapping by means of a dynamic Spatial Light Modulator (SLM). Actually, the DEP trapping of graphite particles onto photorefractive substrates has been already demonstrated through SLM projection.[22] However, only hybrid crystal/PDMS systems were obtained with no *in situ* reconfigurability. In fact, the channel was fabricated separately by conventional replica moulding and successively attached onto the photorefractive crystal. Conversely, we demonstrate here an all-optical approach where the forces generated on the LN crystal surface by the photorefractive effect are used for actuating[23] the liquid curable polymers (*i.e.* PDMS) that build the desired microfluidic PDMS channel structures directly onto the same crystal. Once the PDMS is cured, particle trapping is performed in the channel *via* DEP forces. The particle trapping into the built-in channel structures is achieved by reconfiguring easily the geometry of the photorefractive effect through the SLM light projection. The possibility of addressing specific functionalities, through the dynamic flexibility offered by light projection directly onto lab-on-a-chip devices, provides important advantages, as shown recently by different achievements where the concept of "reconfigurability" was exploited thoroughly.[24] Moreover, the *in situ* realization of the channels makes the approach more rapid, cost-effective and versatile since no mould fabrication and replication are required. The geometry of the channel can be realized with more versatility through simple reconfiguration of the optical light pattern. Even though the adherence of PDMS to most glass and photorefractive substrates is well known, the built-in channels presented here may help to prevent the potential leakage effects at the PDMS/crystal interface. Furthermore, by using the same photorefractive pattern for channel formation and for particle trapping, this approach provides the additional capability of aligning microparticles precisely along the channel borders, which could be desirable in peculiar applications. In fact, such alignment would be much more difficult in the case of hybrid crystal/PDMS systems. In previous work[21] we demonstrated the possibility of fabricating microstructures by using the space charge fields generated on iron doped LN crystals. Therein we fabricated gratings into PDMS layers deposited onto the surface of LN wafers by a whole optical process that we named Light Induced Patterning (LIP). The main drawback of LIP is the limited amount of reliable geometries. Indeed, the shape of the realized microstructures depended on the amplitude grating inserted in the light optical path. We made one and two dimensional gratings and the possibility of generating more complex shapes was mentioned.

In the present paper we show that it is possible to overcome the limitations imposed by the LIP method in terms of light-pattern flexibility. Moreover, the main idea of the present work is to demonstrate that such PDMS structures can be used as microfluidic devices. In particular, we demonstrate the possibility of making PDMS chambers and channels in which particles can be trapped by the DEP effect. The improvement in terms of technology is given by the SLM that is inserted in the optical apparatus replacing the amplitude grating employed in the setup described in ref. 21 but most importantly the flexibility of the holographic SLM projection technique allows the design and realization of the DEP trapping with, in principle, any geometric configuration. The material that allows the realization of our device is the iron-doped LN crystal. Our aim is the fabrication, on its surface, of PDMS microstructures suitable to be used as microchannels. The second step is the trapping of microparticles inside this channel. Both the realization of PDMS structures and the trapping experiments are based on the physics of the photorefractive effect in LN crystals. DEP forces, induced on the LN surface, depend on the intensity profile of laser light patterns. The possibility of designing the light in arbitrary ways is given by the SLM employed in microchannel fabrication as well as in particle trapping.

Materials and methods

We use *x*-cut Fe^{2+3+} doped (0.05% weight) LN crystals whose thickness is 500 μm and linear dimensions in the *y* and *z* directions are 1 × 1 cm^2. The first part of the experiment deals with the fabrication of channels on the LN surface. The material used to fabricate the channel is a polymeric liquid, the PDMS, that is spun onto the LN surface.

The crystal substrate is coated with a PDMS layer by a conventional spin-coater for 2 min at 9000 RPM in order to get a thin and uniform PDMS film over the *x* crystal face. The sample, made of LN and PDMS, is positioned in the optical setup as sketched in Fig. 1(a).

The light source is an argon laser emitting at 514 nm, the beam is linearly polarized by a wave plate ($\lambda/2$) and expanded to fill the aperture of the SLM (phase only SLM - Pluto VIS Holoeye). The light reflected by the SLM is collected by a lens (focal length f = 30 cm) and projected in the plane where the sample is positioned. A second wave plate is positioned before the crystal. The polarization is an important parameter to be controlled so the first wave plate is used to get the maximum efficiency from the SLM while the second one is necessary to enhance the efficiency of the photorefractive effect in the crystal. The distance between the SLM and the lens equals that between the lens and the crystal sample, *i.e.* the focal length *f*. Due to this arrangement, the complex wavefield in the SLM plane is the Fourier transform of the complex wavefield in the sample plane and *vice versa* (Fig. 1(b)). The SLM is a reconfigurable diffractive optical element, actually a matrix of 1920 × 1080 pixels of 256 grey levels, a phase hologram driven in real time by computer control. The flexibility introduced by the SLM is fundamental as any desired light pattern in the sample plane can be realized by managing the field distribution just after reflection on the SLM device. The matrix displayed on the SLM is named Computer Generated Hologram (CGH). Several algorithms exist to best evaluate the CGH as different light intensity profiles need different numerical solutions.[25–29] Usually, the SLMs are used

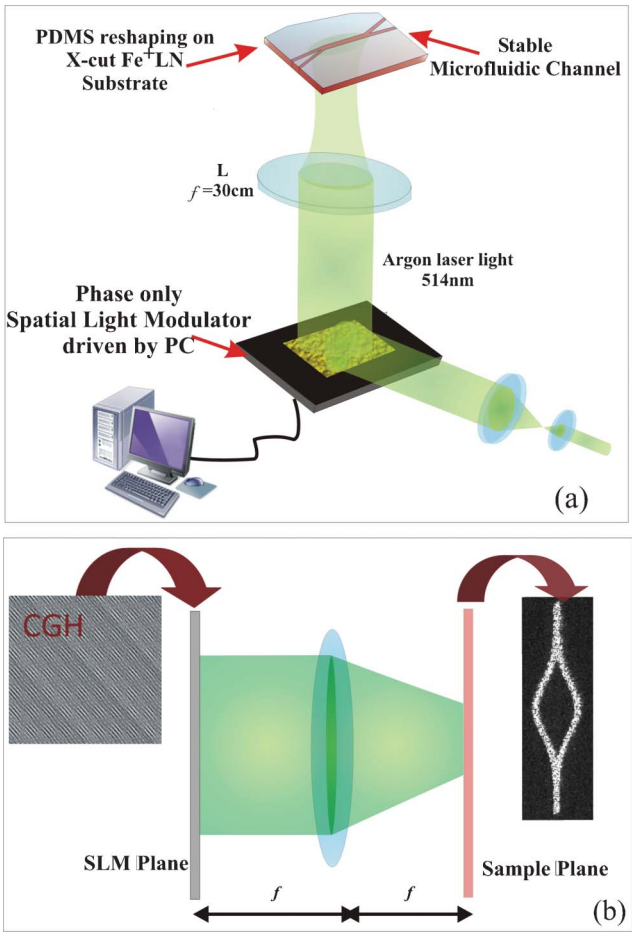

Fig. 1 (a) Experimental arrangement for the PDMS patterning, (b) the SLM plane and the sample plane are conjugated (Fourier configuration).

for generating light intensity distributions able to trap micro-particles in chambers and these kinds of experiments need the generation of discrete light patterns (the trapping sites). Here, we encounter a different issue, *i.e.* the generation of a continuous profile able to induce the PDMS reshaping onto the LN surface.

Experimental results

Channels fabrication

In the first step of the work we implement an algorithm to improve the efficiency and the smoothness of the desired profiles. Our algorithm belongs to the group of Iterative Fourier Transform Algorithms (IFTA),[25–27] a numerical target of the designed intensity pattern is the input and the correspondent output is the CGH to be displayed on the SLM. Fig. 2 shows an example of a possible light distribution. In particular, Fig. 2(a,b) present the numerical target and the actual light distribution in the sample plane before inserting the crystal. The image is recorded by a CCD camera and the laser light profile presented is a quite smooth shape without holes, steps or discontinuities. As sketched in the setup of Fig. 1(a), the LN sample with the PDMS layer is positioned in the conjugate plane of the SLM where the desired light distribution is displayed (Fig. 2(b)). The laser power, impinging on the sample, is about 500 mW and its polarization is in the direction of the *z*-axis of the crystal. A transparent hot plate is positioned under the sample in order to cure the polymer after the reshaping induced by the light exposure.

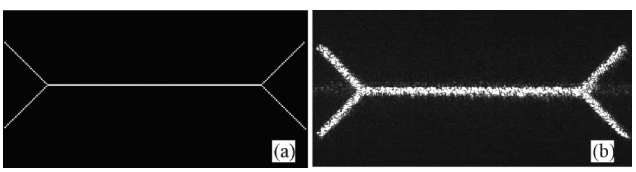

Fig. 2 (a) Numerical ideal target given as input to the algorithm, (b) real laser light display in the sample plane.

The illumination excites the charge carriers inside the LN crystal, the generated space-charge field[28–32] modulates the refractive index *via* an electro-optic effect thus forming a phase distribution inside the crystal, that depends on structured intensity laser light (Fig. 2(b)). The space-charge field inside the material generates, on the upper surface, DEP forces able to pattern the liquid PDMS film as extensively explained in ref. 21. The PDMS reshaping starts just after the light is switched on. The liquid polymer tends to concentrate across the illuminated regions, draining away from the dark regions. For example, by using the target displayed in Fig. 2 we cannot obtain a double-y-shaped channel but its negative counterpart. So the target design is the second issue of the presented work. Several targets have been studied to realize different geometries for the PDMS reshaping. Images of the realized channels are displayed in Fig. 3, some pictures are recorded in bright field microscopy and others by stereomicroscope. As can be seen from Fig. 3 the channels have different linear dimensions (*y* and *z* directions). Both the geometry and the dimensions are controlled by managing the algorithm for the CGH generation. The feature common to all the devices is that the channel walls are made of PDMS directly written onto the LN substrate. This feature allows, as it will be proved in the following, the trapping of particles in the channels. The devices reported in Fig. 3 are obtained after curing the PDMS. Indeed, once the structure is formed a rapid PDMS curing is achieved by switching the hot plate on. The procedure is quick and easy to replicate. The entire fabrication process takes one hour and it needs only one fabrication step, *i.e.* the illumination of the sample by structured laser light. The channel length reported in this paper ranges between 500 μm and 3 mm, while the width ranges between 10 μm and 100 μm, and the channel walls are a few microns (2 μm–10 μm) high, depending on the thickness of the liquid layer deposited on the LN substrate. As said before, the length and the width are managed numerically by the design of the target after calibration is accomplished.

DEP trapping of MWCNTs

In the second step, we demonstrate the possibility of trapping microparticles in the channels fabricated by the LIP method. The field pattern recorded in the crystal to assemble the PDMS is erased in order to avoid the particle trapping around the PDMS channel walls. The structure, made of PDMS and LN, is covered by a coverslip squeezed on it by a home-made device. A mixture of carboxyl oil (carboxylic acid - $C_5H_{10}O_2$) and multiwall carbon

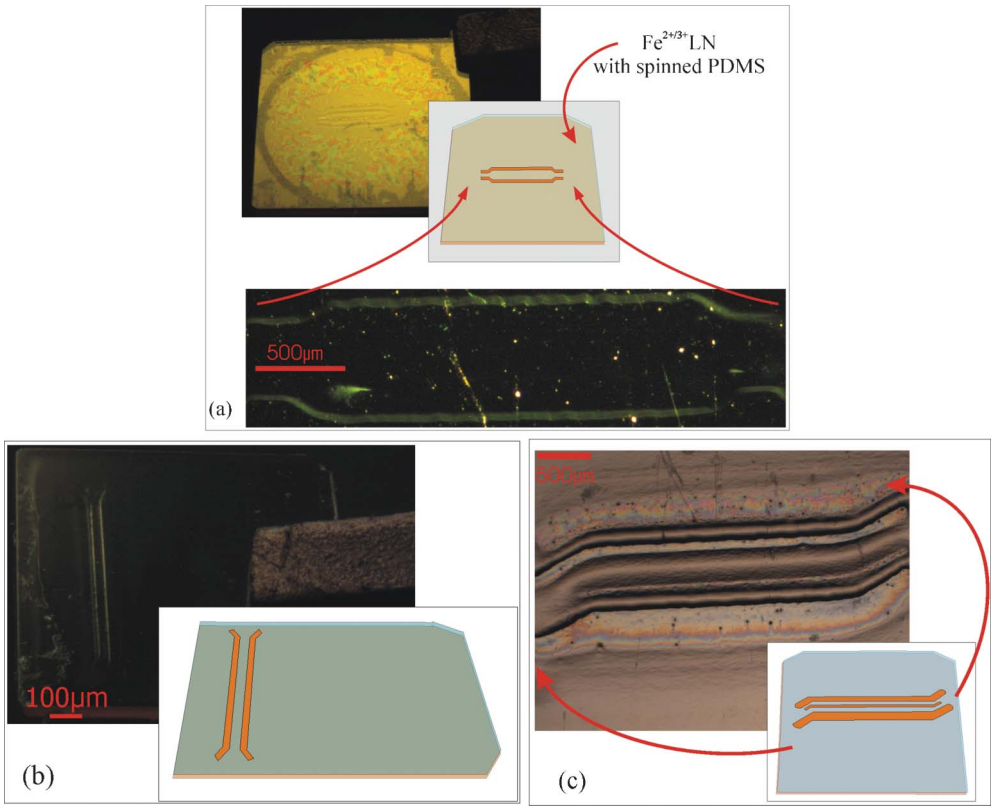

Fig. 3 Examples of PDMS microchannels obtained designing the intensity target and recovering the corresponding CGH. (a) and (b) stereomicroscope images; (c) bright field microscope images.

nanotubes (MWCNTs) (produced by chemical vapor deposition and supplied by Aldrich Chemistry with inner and outer diameters of about 110–170 nm, respectively, and length in the range of 5–9 μm) is introduced in the channel through the final part of the channel not covered by the coverslip. The final step is the positioning of the sample in the laser path following the scheme shown in Fig. 1(a,b). As for the previous fabrication process, the space-charge field inside the material generates, on the upper surface, DEP forces, but, unlike previously, the light impinging on the sample is structured to trap microparticles. In a non-uniform electric field, the induced dipole experiences a net force

$$\vec{f}_{\mathrm{DEP}} = (\vec{p}\cdot\vec{\nabla})\vec{E} \tag{1}$$

where $p = 4\pi\varepsilon_1 R^3[f_{\mathrm{CM}}(\omega)]E$is the induced electric dipole for a spherical particle of radius R immersed in the electric field $E$and $[f_{\mathrm{CM}}(\omega)]$ is the real part of the Clausius–Mossotti factor, whose form is:

$$f_{\mathrm{CM}}(\omega) = \frac{\tilde{\varepsilon}_2 - \tilde{\varepsilon}_1}{\tilde{\varepsilon}_2 + 2\tilde{\varepsilon}_1} \tag{2}$$

where $\tilde{\varepsilon}_i = \varepsilon_i + i\sigma_i$ (i = 1, 2) represent, respectively, the complex permittivity of liquid medium and particle.

The light impinging on the sample is structured in order to form a grating inside the channel. The MWCNTs are trapped following the grating pattern. Fig. 4 shows the trapping effect inside the channel. The initial part, shown in the inset of Fig. 4(a), is used to insert the mixture inside and is not covered by the coverslip. Two photorefractive gratings are inscribed in the crystal in correspondence with two channel areas. While the mixture is flowing inside, the MWCNTs are trapped in correspondence with the photorefractive gratings. In Fig. 4(b)

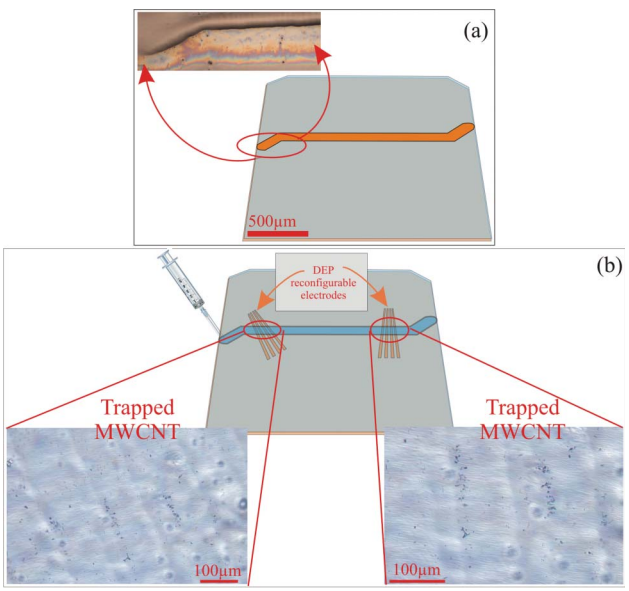

Fig. 4 (a) A coverslip over the reshaped PDMS closes the channel chamber, except for where the mixture is injected, (b) the MWCNTs are trapped in two regions and arranged following the geometry of the photorefractive grating inscribed in the LN crystal.

the positioning and orientation of the grating are displayed, together with the bright field images of the observed phenomenon. MWCNTs are trapped at the end parts of the channel, likewise they can be trapped at any position along it. Indeed, as shown in Fig. 5, a photorefractive grating is inscribed inside the LN crystal in order to trap particles along the whole channel.

Fig. 5 shows a further demonstration of the trapping capabilities in a channel different from that of Fig. 4. The photorefractive grating is clearly visible and the MWCNTs are collected in correspondence with the boundary between the dark and the bright regions. The inset is an image of the channel before injecting the mixture. We chose a mixture of MWCNTs in carboxyl acid as the differences between their dielectric constants assure a better DEP response for CNT trapping.

DEP chaining of graphite

As an additional experiment we adopted graphite nanofibers, (width × length, 50–250 nm × 0.5–5 μm) dispersed into the same oily buffer (carboxylic acid). Then the liquid was introduced into the microfluidic channel where a set of DEP traps were created almost perpendicularly to the longitudinal direction of the channel itself. Interestingly the graphite nanofibers experience a sort of chaining effect. The chaining effect of microparticles is not new. In fact, it has been observed in different conditions and also with various types of nano and microparticles. For example, it has been observed that gold nanoparticles form a sort of pearl-chain at electrode gaps driven by the DEP forces.[33] The non-uniform electric fields induce the electric polarization with a dipole–dipole interaction between particles thus boosting the formation of chains. Fig. 6 shows clearly how multiple, very long chains of graphite fibers are trapped by the photorefractive DEP forces and are positioned perpendicularly to the DEP charge electrodes. In the supplementary movie† it can be seen how the process of accumulation of fiber takes place while the liquid flows into the channel.[34] This last experiment evidences how the electric field gradients generated by the photorefractive effect induce the self-assembly of graphite nanofibers into intriguingly very long chains. Graphite nanofibers exhibit a different behaviour in comparison with CNTs. This is due to the higher value of the graphite dielectric constant which is able to induce dipole–dipole interaction and, consequently, chains form.

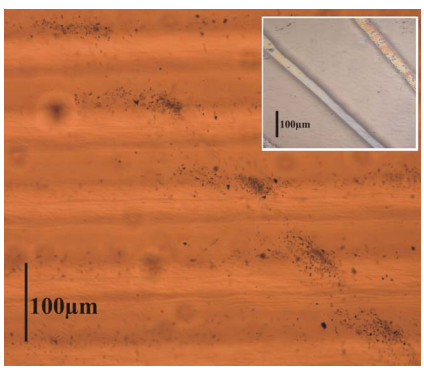

Fig. 5 MWCNTs trapped inside the PDMS channel by photorefractive grating.

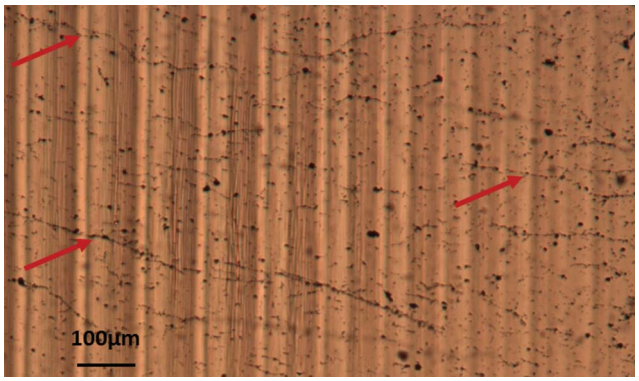

Fig. 6 Graphite chains obtained by exploiting the photorefractive grating inscribed in the iron doped LN crystal.

Conclusions

An all-optical and electrode-free approach is presented here for achieving reconfigurable DEP particle trapping into microfluidic chips. The geometrical configuration of the DEP traps can be changed in an all-optical mode by writing/erasing steps making the chip flexible and versatile. The results reported here open a novel route to design and apply dynamic on-chip DEP traps just driven by light exposure. The flexibility of an SLM device would allow in principle the configuration of any light shape/pattern to create invisible electrodes on-chip. Moreover, we have shown the feasibility in the fabrication of PDMS microfluidic channels with diverse geometrical configurations. Such microfluidic channels are fabricated by exploiting photorefractive light induced forces so they are directly integrated on-chip. The light induced virtual electrodes have been realized on the ferroelectric substrate in different locations and with different orientations. In addition we have verified positive DEP trapping of MWCNTs and an interesting trapping and self-assembling of chaining graphite nanofibers.

References

1 A. T. J. Kadaksham, P. Singh and N. Aubry, *Electrophoresis*, 2004, **25**, 3625–3632.
2 J. Chen, J. Li and Y. Sun, *Lab Chip*, 2012, **12**, 1753–1767.
3 K. Khoshmanesh, S. Nahavandi, S. Baratchi, A. Mitchell and K. Kalantar-zadeh, *Biosens. Bioelectron.*, 2011, **26**, 1800–1814.
4 F. E. H. Tay, L. M. Yu and C. Iliescu, *Def. Sci. J.*, 2009, **59**, 595–604.
5 K. Yamamoto, S. Akita and Y. Nakayama, *Jpn. J. Appl. Phys.*, 1996, **35**, 917–918.
6 K. Yamamoto, S. Akita and Y. Nakayama, *J. Phys. D: Appl. Phys.*, 1998, **31**, 34–36.
7 K. Khoshmanesh, C. Zhang, S. Nahavandi, F. J. Tovar-Lopez, S. Baratchi, Z. Hu, A. Mitchell and K. Kalantar-zadeh, *Electrophoresis*, 2010, **31**, 1366–1375.
8 R. H. M. Chan, C. K. M. Fung and W. J. Li, *Nanotechnology*, 2004, **15**, S1–S6.
9 K. Park, H. J. Suk, D. Akin and R. Bashir, *Lab Chip*, 2009, **9**, 2224–2229.
10 W. A. Braff, A. Pignier and C. R. Buie, *Lab Chip*, 2012, **12**, 1327–1331.
11 Y. H. Lin, Y.W. Yang, Y. D. Chen, S. S. Wang, Y. H. Chang and M. H. Wu, *Lab Chip*, 2012, **12**, 1164–1173.
12 A. Jamshidi, P. J. Pauzauskie, P. J. Schuck, A. T. Ohta, P.-Y. Chiou, J. Chou, P. Yang and M. C. Wu, *Nat. Photonics*, 2008, **2**, 86–89.
13 H. A. Eggert, F. Y. Kuhnert, J. R. Adleman, D. Psaltis and K. Buse, *Appl. Phys. Lett.*, 2007, **90**, 241909, 1–3.

14 L. Miccio, A. Finizio, S. Grilli, V. Vespini, M. Paturzo, S. De Nicola and P. Ferraro, *Opt. Express*, 2009, **17**, 2487–2499.
15 S. Grilli and P. Ferraro, *Appl. Phys. Lett.*, 2008, **92**, 232902.
16 S. Grilli, V. Vespini and P. Ferraro, *Langmuir*, 2008, **24**, 13262–13265.
17 P. Ferraro, S. Coppola, S. Grilli, M. Paturzo and V. Vespini, *Nat. Nanotechnol.*, 2010, **5**, 429–435.
18 S. Coppola, V. Vespini, S. Grilli and P. Ferraro, *Lab Chip*, 2011, **11**, 3294–3298.
19 S. Grilli, S. Coppola, V. Vespini, F. Merola, A. Finizio and P. Ferraro, *Proc. Natl. Acad. Sci. U. S. A.*, 2011, **37**, 15106–15111.
20 X. Xi, D. Zhao, F. Tong and T. Cao, *Soft Matter*, 2012, **8**, 298–302.
21 L. Miccio, M. Paturzo, A. Finizio and P. Ferraro, *Opt. Express*, 2010, **18**, 10947–10955.
22 M. Esseling, F. Holtmann, M. Woerdemann and C. Denz, *Opt. Express*, 2010, **18**, 17404–17411.
23 T. B. Jones, M. Gunji, M. Washizu and M. J. Feldman, *J. Appl. Phys.*, 2001, **89**, 1441–1448.
24 M. Krishnan and D. Erickson, *Lab Chip*, 2012, **12**, 613–621.
25 R. W. Gerchberg and W. O. Saxton, *Optic*, 1972, **35**, 237–246.
26 R. Di Leonardo, F. Ianni and G. Ruocco, *Opt. Express*, 2007, **15**, 1913–1922.
27 E. R. Dufresne, G. C. Spalding, M. T. Dearing, S. A. Sheets and D. G. Grier, *Rev. Sci. Instrum.*, 2001, **72**, 1810.
28 M. Hesseling, M. Woerdemann, A. Hermerschidt and C. Denz, *Opt. Lett.*, 2011, **36**, 3657–3659.
29 M. Montes-Usategui, E. Pleguezuelos, J. Andilla and E. Martin-Badosa, *Opt. Express*, 2006, **14**, 2101–2107.
30 K. Buse, *Appl. Phys. B: Lasers Opt.*, 1997, **64**(3), 273–291.
31 F. Argullo-Lopez, G. F. Calvoand M. Carrascosa, "Fundamentals of Photorefractive Phenomena" in *Photorefractive materials and their applications I*, ed. P. Gunter and J. P. Huignard, Springer, 2006, pp. 43–82.
32 M. Luennemann, U. Hartwig and K. Buse, *J. Opt. Soc. Am. B*, 2003, **20**(8), 1643–1648.
33 R. Kretschmer and W. Fritzsche, *Langmuir*, 2004, **20**(26), 11797–11801.
34 O. E. Nicotra, A. La Magna and S. Coffa, *Appl. Phys. Lett.*, 2009, **95**, 073702.